Direct Torque Controller of SRM for EV Application Based on Neural Network

Anuradha Devi Tellapati[1](✉), Malligunta Kiran Kumar[2], Natarajan Karuppaiah[1], S. Ravi Teja[2], and Kambhampati Venkata Govardhan Rao[3]

[1] Department of Electrical and Electronics Engineering, Vardhman College of Engineering, Shamshabad, Hyderabad, Telangana, India
anuradhadevi.eee@gmail.com

[2] Department of Electrical and Electronics Engineering, Koneru Lakshmaiah Education Foundation, Vaddeswaram, Guntur, A.P., India

[3] Department of Electrical and Electronics Engineering, St. Martin's Engineering College, Secunderabad, Hyderabad, Telangana, India

Abstract. This paper presents the machine learning based control of cascaded converter fed SRM drive of electric vehicle. The electric vehicle which is driven by a 6/4 Switched Reluctance Motor (SRM) powered by four battery banks is considered in this paper. The new topology of converter is proposed to drive SRM effectively for application of electric car. The direct torque controller is implemented with the help of neural network for effective speed controller with minimum ripples in electromagnetic torque. The required pulses are generated with space vector Pulse Width Modulation (PWM) technique. The electromagnetic torque generated by SRM needs to be maintained at ripples free for smooth operation of electric car. The mathematical validation is implemented to achieve the required power rating of SRM for Toyota Car. The proposed topology of converter has a facility of using four battery banks, hence the charging time of batteries will be minimized. The direct torque controller with model reference adaptive controller is implemented for establishing sensor less operation. The proposed system is implemented in MATLAB/Simulink. The extensive results are presented which validate the proposed system for steady state and transient state requirements of the drive.

Keywords: Electric Car · Direct Torque Control · SRM · SVPWM

1 Introduction

Global warming is creating many major problems in worldwide with the increasing consumption of fossil fuel. However, the use of fossil fuel is increasing day by day. The major share in consumption of fossil fuel is utilizing for transport and unfortunately fossil fuels are limited which leads to increasing price day by day. Hence, worldwide researchers are searching for an alternative solution and developing electric vehicles

X. Cheng (Ed): BROADNETS 2024, LNICST 602, pp. 58–69, 2025.
https://doi.org/10.1007/978-3-031-81171-5_6

which can reduce carbon emissions to protect nature from pollution [1, 2]. Generally, cars are using by many people and it is becoming and fascinate vehicle in our life. Moreover, utilization of cars is increasing day-by-day and diesel/petrol cars are becoming major sources of pollution. Therefore, electric cars need to be developed for fulfill our transportation needs. The design, manufacturing and usage of electric vehicles started long back throughout the world. SRM proved as a good companion for electric vehicle drive for it simple construction and torque capacity. However, it is the converter and controller that decides the robustness of drive.

A review of comparison between different power electronic converters for SRM drives such as asymmetric converter, H-bridge type converter, C-Dump type converter, R-Dump type converter, variable voltage at dc link and three phase bridge module converters were reported [3, 4]. The results show that the asymmetric converter produces better results for SRM. The detailed analysis SRM by using different types of converters were discussed. The asymmetric converter provides better results compared to the other type of converters and the converter has the bridge circuit at the input side which in turn increases the conduction losses [5–7]. A regeneration mode of SRM which was examined by using C-Dump converter and the energy recovery mechanism. The braking mode control was achieved by dynamically adjusting the excitation reference as a control variable [8]. A negative torque generation model of asymmetric converter which to reduce the torque ripple of by high magnetization & demagnetization voltage. But the cost is increased due to the boost capacitor & diodes in the input side [9, 10].

With these findings, a novel converter with novel control for SRM drive is presented in this paper. Rest of the paper is organized as follows. Section 2 presents description of the system, Sect. 3 presents sizing of components, Sect. 4 presents controller model, Sect. 6 presents results and discussion and finally conclusions are presented.

2 System Description

The schematic of the proposed cascaded converter based SRM drive for electric vehicle is shown in Fig. 1. The new topology of converter is implemented which provides reliable voltage waveform owing to its cascaded structure. Apart from many controllers, Direct Torque Controller (DTC) is having high priority to operate motor under fewer ripples in torque. Therefore, DTC is employed along with Space Vector Pulse Width Modulation (SVPWM) for effective control of SRM. To reduce ripples in torque and smooth operation of speed, the artificial neural network (ANN) is developed. The new topology of converter can have facility to divide all batteries in four battery banks. This can provide felicity to adjust battery banks at different places in car according to availability of space. An optimized ANN based direct torque control is employed for the EV drive. The direct torque control is selecte4d for the reasons of quick response and independent torque and speed control. An improved ANN networked was used to determine control parameters for DTC. Speed was estimated using model resonance adaption technique.

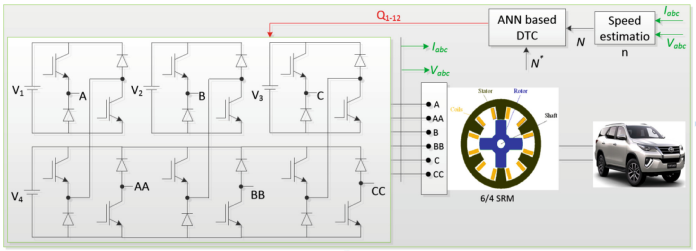

Fig. 1. Proposed System in Electric Vehicle with SRM

2.1 Modeling of the Battery

Battery energy storage is important part of the electric or hybrid electric vehicle. The proper controller with precious energy management system is needed for enhancing charge cycles which shall supervise for proper charge and discharge sequence. The battery bank used in EV usually consists of series connected battery to establish required rated voltage. Therefore, current flowing through all individual batteries is same during both charging and discharging. However, in order to achieve unique flow of current through all batteries, active balancing of the system is required which ensures equal charging or discharging among the cells in the battery pack.

The state of the charge (SOC) of the complete battery bank is measured and stored for the controlling purpose. A generic model of the battery bank is implemented from [11–13] in this paper. The parameter of temperature is also considered for more realistic in this implantation. The basic controlled voltage dependent source is described through following basic expressions.

$$E_m = E_{m0} - K_E(273 + \theta)(1 - SOC) \tag{7}$$

$$Q_e(t) = Q_{e\_init} + \int_0^t -I_m(\tau)d\tau \tag{8}$$

$$I_p = V_{PN} G_{P0} \exp\left(\frac{V_{PN}}{V_{P0}(\tau_P s + 1)} + A_P\left(1 - \frac{\theta}{\theta_f}\right)\right) \tag{9}$$

$$C(I,\ \theta) = \frac{K_c C_{0*} K_t}{1 + (K_c - 1)\left(I / I^*\right)^{\delta}},\ K_t = LUT(\theta) \tag{10}$$

where,

$$SOC = 1 - \frac{Q_e}{C(0,\ \theta)}\ ,\quad DOC = 1 - \frac{Q_e}{C\left(I_{avg},\ \theta\right)}, \theta(t) = \theta_{init} + \int_0^t \frac{\left(Ps - \frac{(\theta - \theta_a)}{R_\theta}\right)}{C_\theta} d\tau$$

symbols are denoted as follows:

Q_e - extracted charge; Q_{e_init}- intial extracted charge; I_m – current deliverd; τ – time variable; I_P- parasitic current; V_{PN}- parasitic voltge (Figs. 2 and 3).

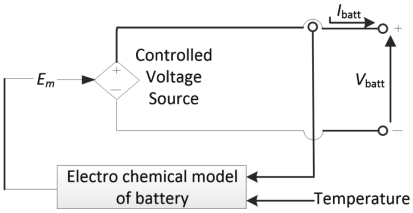

Fig. 2. Generic Battery Model

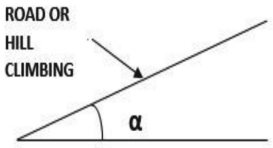

Fig. 3. Angle between the slope and the flat surface

3 Sizing of System Components

The Toyota EV [14] was considered for sizing the SRM drive. The technical details pertaining to weight [15], coefficients etc. was taken from [16, 17].

This section presents the sizing of following components of the drives:

- Power required by load [18, 19]
- Sizing of motor
- Sizing of battery

3.1 Load Power Sizing

The required tractive force is given as:

$$F_{total} = F_{rolling} + F_{gradient} + F_{aerodynamic} \tag{11}$$

where, F_{total} = Total force; $F_{rolling}$ = Rolling Resistance force; $F_{gradient}$ = Gradient Resistance force; $F_{aerodynamic}$ = Aerodynamic drag force.

A. **Tractive force for C_{rr}:** It is the resistance offered by the road due to the friction between tyres and road. To calculate the force offered by rolling resistance the following formula is used given in Eq. (12).

$$F_{rolling} = C_{rr} \times M \times g \tag{12}$$

where, C_{rr} = Rolling resistance coefficient; M = mass in kg; g = acceleration due to gravity = 9.81 m/s^2; For the application considered, Crr = 0.01; M = 3000 kg;

Therefore,

$$F_{rolling} = 294.30\,\text{N}$$

Required power to overcome the rolling resistance of 294.30 N is:

$$P_{rolling} = F_{rolling} \times \frac{V}{3600} = 6.20\,\text{kW}$$

B. **Tractive force for gradient:** Gradient resistance is the resistance offered by a slope surface while climbing a fly-over or hill. α is the angle between the slope and the flat surface as shown in Fig. 1.

The gradient resistance can be calculated by using the formula given in Eq. (13):

$$F_{gradient} = \pm M \times g \times \sin\alpha \tag{13}$$

$$F_{gradient} \text{ at } 6^\circ \text{ is } = 1538\,\text{N}.$$

$$P_{gradient} = F_{gradient} \times \frac{V}{360} = 10.2\,\text{kW}$$

C. **Tractive force for C_A:** It can be determined by the vehicle shape. The aerodynamic drag is calculated by using the formula given in Eq. (14):

$$F_{aerodynamic} = 0.5 \times C_A \times A_f \times \rho \times (V + V_0)^2 \tag{14}$$

One more force due to inertia also acts on the vehicle during acceleration and deceleration. In this work, the total power required to compensate all the resistive forces and drag is taken as 2.6 kW.

Thus, a 20-kW load power is calculated to meet all the above components of the load resistance and for required torque at nominal load of the vehicle.

3.2 Battery Pack Sizing

Section 2 presented the model for the battery which showed the significance of C-rate, initial charge, and chemistry for estimated power delivery and lifetime. Lead acid batteries vs Li-ion chemistry depends on economics of the drive [20, 21]. First one for low cost and second one for higher energy density. This section presents size of the batter pack required for meeting the 20-kW nominal load.

$$I_{Ah} = \frac{Power \times Time}{Voltage} = \frac{20000 \times 4.5hr}{300} = 300Ahr \tag{15}$$

3.3 SRM Sizing

SRM as stated in Sect. 1 provides high torque-to-ampere ration, superior control, and allows for smooth commutation. The immediate supplier to the load being 6/4 pole SRM, the power sizing of the SRM shall be 20 kW as nominal value. The A 400 V voltage limits the required current to around 20 A, thus could result in simple insulation requirement. However, the inertia of the motor shall be small to serve quick transient requirements [22–24]. Therefore, the windings with good aligned inductance and with less copper requirement shall make the inertia requirement possible. Also, the losses in the motor phase windings should be limited to 0.1 % of the total power rating. Thus, a lighter SRM with high torque capability is the resulting choice for motor.

The SRM parameters which are considered for drive provided in Table 1:

Table 1. SRM Parameters

S. No	Parameter	Value
1	Nominal Rated Power	20 KW
2	Nominal line to line Voltage	400 V
3	Stator Resistance (Rs)	0.7384
4	Stator Inductance (Lls)	0.003045
5	Inertia (J)	0.0343
6	Pole Pairs	6/4

4 Controller of SRM

The 6/4 pole 20 kW SRM is operated cascaded converter with the following control algorithm.

The objectives of Control are:

- Effective and accurate tracking for change in speed command
- Speed regulation for load change
- Quick transient interval for reverse command
- Zero steady state error for motor speed command

The control scheme includes the following salient aspects:

- The control does not require sensing of speed as this was achieved through model reference adaptive control for estimation of speed
- Machine learning for deriving torque command from speed error
- Space vector modulation for gating pulse generation

The stated objectives necessiate d-q model of the SRM for determining torque and flux commands which was stated in Eqs. (16) and (17).

$$[(1-\sigma)T_s + T_r]\frac{d}{dt}\psi_{r\alpha} = \frac{L_m}{R_s}u_{s\alpha} - \psi_{r\alpha} - \omega T_r \psi_{r\beta} - \sigma L_m T_s \frac{d}{dt} i_{s\alpha} \tag{16}$$

$$[(1-\sigma)T_s + T_r]\frac{d}{dt}\psi_{r\beta} = \frac{L_m}{R_s}u_{s\beta} - \psi_{r\beta} + \omega T_r \psi_{r\alpha} - \sigma L_m T_s \frac{d}{dt} i_{s\beta} \tag{17}$$

where:

L_s and L_r *are* stator and rotor self-inductance [in H] respectively

L_m = motor magnetizing inductance [in H]

R_r *and* R_s are denoted for rotor and stator Resistance [in Ohm] respectively

ω = Angular speed of the rotor[in rad.s-1]

The purpose of designing DTC is to control independently the direct-axis stator current i_{sd} and the quadrature-axis stator current i_{sq}. But unfortunately, the stator voltage components are in decoupled in nature. That means, the direct axis component u_{sd} and i_{sq} as well as quadrature axis component u_{sq} and i_{sd} are in coupled by depending on

each other. Further, the i_{sd} and i_{sq} should be controlled independently (with decoupled control) if the stator voltage equations are decoupled and the stator current components i_{sd} and i_{sq} are indirectly controlled by controlling the terminal voltages of the motor.

The scheme for model reference adaptive control is shown in Fig. 4(a) and respective SRM motor speed estimation is depicted in Fig. 4(b). Usually sensing the speed by sensors are not preferable due to malfunctions of sensors, needs to provide extra protection and also costly. The block diagram for implementation of SMC for proposed system is shown in Fig. 5. The speed estimated through SMC based MRAC is compared to reference speed and the difference is provided as input to machine learning algorithm which is state in next section. The flux and torque commands generated by machine learning algorithm generates the voltage refence vector for subsequent sample. Then SVPWM technique generates appropriate pulses instantly based on sector. The scheme for identification of sectors, dwell time calculation and transforming in to gating pulses is depicted in Fig. 6. The generated pulses will go to respective switch of converter to produce required output accordingly load and reference speed of SRM.

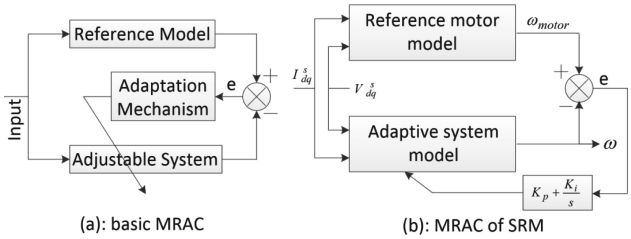

Fig. 4. Estimation of speed using MRAC model of SRM

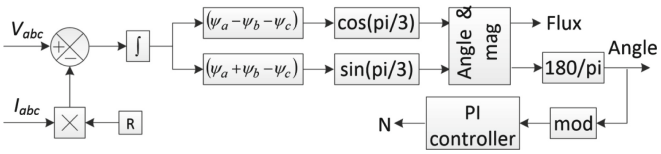

Fig. 5. Implementation of SMC of proposed system

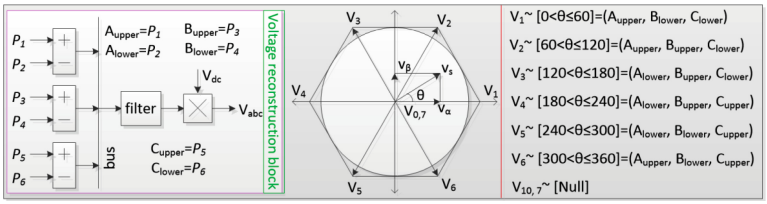

Fig. 6. Space Vector PWM strategy

4.1 Implementation of ANN

Generally artificial intelligent (AI) strategies are a simple computer-oriented programming applications to think and act brilliantly for taking decisions very sharply. To accomplish this objective, the machine learning through artificial neural network (ANN) was employed. The targeted output or results are always produced on the basis of adjusting weight factors accordingly neurons and its corresponding inputs neurons for every cycle in training structure of any neural network design model. The basic process of learning is depicted in Fig. 7 and the corresponding ANN implementation has been considered in this paper. The designed ANN can have ability to adjust their gains by learning process for any disturbance.

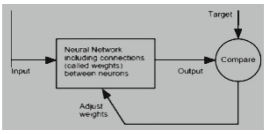

Fig. 7. ANN –Training Structure

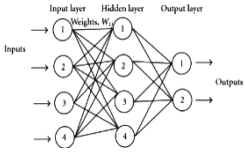

Fig. 8. Feed forward ANN

The basic learning process of the ANN system can be patterns subsequent based on response. Feed-forward ANNs are a very frontward- customary technique, The multilayer of ANN is depicted in Fig. 8. Moreover, due to existing of hidden layer, the controller can exhibit smooth controlling output during large variations in inputs.

Table 2. ANN Parameters

S. No	Parameter	Value
1	Activation Function	Sigmoid
2	Number of Hidden Layers	2
3	Input layers	1
4	Output variables	1
5	Error Bound	0.01
6	Pole Pairs	6/4

5 Results and Discussion

The proposed converter and control for SRM drive are tested in MATLAB/SIMULINK. This section presents the simulation results and observations. The parameters for motor presented in Table 1, ANN parameters presented in Table 2 are utilized for simulation. Other simulation parameters are provided in Table 3.

The simulation results are presented for three scenarios viz. Response of torque and speed for change in load on the vehicle, response pf torque and speed for change in

Table 3. Simulation Parameters

S. No	Parameter	Value
1	Battery Pack Voltage	100 V
2	Battery Packs capacity	P1, P2, P3: 50 AH, P4: 150 AH
3	Power Switches	IGBT: 600 V, 300 A
4	Power Diodes	600 V, 300 A
5	SRM Aligned Inductance	20 mH
6	SRM Unaligned Inductance	330 μH

speed command, response of torque and speed for speed reversal command. Following presents obtained results.

Case-1: Change in Load Torque: The load torque is changed to 50 N-m from zero load. Owing to this change in load, a quick settlement in motor developed torque is observed from Fig. 9. Also, at zero load and at changed load which is met by the motor torque, the steady state ripple in the motor torque is observed to be 2 N-m which accounts for reasonable torque ripple with SRM. The transient interval involved in tracking to new load is observed to be 0.1 s as depicted from Fig. 9. The response of the speed for change on load is depicted in Fig. 10. It is observed from Fig. 10 that the transient interval for the speed to settle back to reference speed is 0.5 s which proves the robustness of the proposed machine learning algorithm and direct torque control implementation. Also, there are only few oscillations at the transient which indicates the damping of the system. Power delivered from the battery pack for change in load is shown in Fig. 11. Battery pack c-rate is changed instantly following the change in load and thus supplying the power at increased current as depicted from Fig. 11.

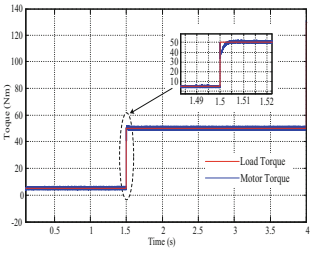

Fig. 9. Tracking of load torque

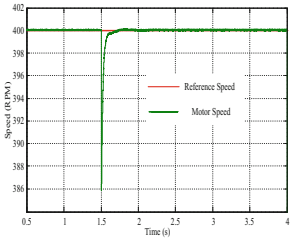

Fig. 10. Response of Speed under Increasing Load Torque

Case-2: Step change in speed command: EV loads demand for quickly changing speed requirements as per the throttle position for given load following various drive cycles. Therefore, the proposed control is tested for a step change in speed command with a magnitude of about 120 rpm. Following the change in speed command, a dip in dc link voltage is observed from Fig. 12 which settled back to reference value with in 05 s. Magnitude of dip pertains to the allowable maximum dip in voltage which

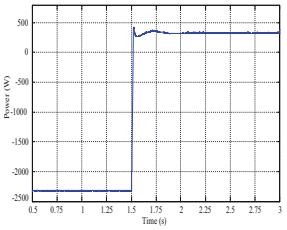

Fig. 11. Battery power dynamics

indicates the robustness of control algorithm. The tracking of speed command is shown in Fig. 13. The transient response presented in Fig. 14 shows the accurate tracking of speed command with zero steady state error and quick interval of 0.05 s. Also, the peak overshoot is marginal as 10 %. The change sis torque owing to speed change is depicted in Fig. 13. Pertaining to change in speed command the torque in transient period is held at maximum to achieve the quick acceleration to new speed and then the torque returns to meet the load which is observed from Fig. 13.

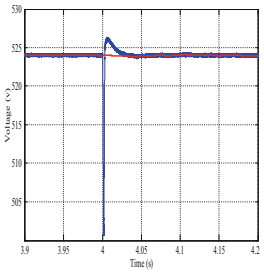

Fig. 12. DC link voltage

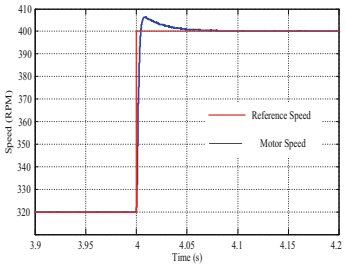

Fig. 13. Response of speed

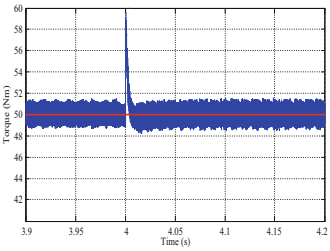

Fig. 14. Torque response for speed change command

Case-3: Reverse driving of the Vehicle: The condition of sudden reversal of speed is simulated. A step change in speed from +80 rpm to −80 rpm was demanded. The response of the speed and drive torque were analyzed. The response of speed as observed from Fig. 15 shows the accurate tracking of new speed with zero steady state error along with a quick transient time of 0.08 s. The dynamics of dc link voltage pertaining to speed reversal is shown in Fig. 16. A sudden dip owing to reversal command is observed and

quick transient time of 0.05 s is observed for settling back to reference value. A sudden dip in drive torque was observed from Fig. 17 during change- over of drive speed to new value owing to the fact that the drive does not hold any load during transient speed reversal which was settled in quick interval of 0.01 s.

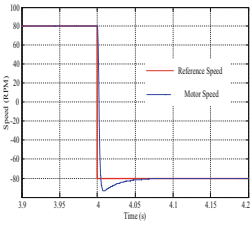

Fig. 15. Reference and motor speed in reverse direction

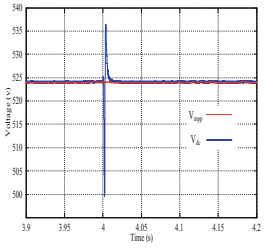

Fig. 16. dc link voltage under change in direction

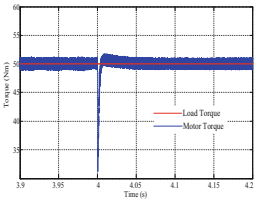

Fig. 17. Torque dynamics for speed change

From the simulation results presented, it is observed that the proposed cascaded converter structure is proved to be reliable with four battery packs supplying the load leading to an improved availability of source for failures in front or rare battery pack modules. The reliability index is increased to 66.67 % which is inly 50 % with conventional asymmetric converter based SRM drive. Then, the efficiency of the conversion is also increased as observed from quick transients of less than 0.5 s for speed and 0.05 s for torque.

6 Conclusion

A novel cascaded converter topology and machine learning based direct torque control of SRM drive for electric vehicle application is presented. The detailed models for load, battery, motor, and converter are discussed. Sizing of all these components was presented. Various stages of control algorithm were discussed which included speed estimation, torque reference generation through machine learning, and current control. The simulation results for steady state torque shown 2 N-m ripple at nominal load. The transients in torque and speed settle with in 0.5 s for any parameter change. The power requirements were met accurately and quickly by proposed battery structure. Thus, the proposed converter and control proved as a good solution for modular drives for SRM based EV drives with robust and efficient control.

References

1. Malla, S.G., et al.: Wind and photovoltaic based hybrid stand-alone power generation system. IEEE: International Conference on Energy, Communication, Data Analytics and Soft Computing (ICECDS 2017). Chennai, India (2017)
2. Malla, S.G., et al.: Solar-hydrogen energy based hybrid electric vehicle. IEEE: International Conference on Energy, Communication, Data Analytics and Soft Computing (ICECDS 2017). Chennai, India (2017)
3. Bose, B.K.: Power Electronics and Motor Drives. Academic Press, Imprint of Elsevier (2006)
4. Theraja, B.L., Theraja, A.K.: A Textbook of Electrical Technology, Vol. 2
5. Porselvi, T., et al.: Selection of power rating of an electric motor for electric vehicles. International Journal of Engineering Science and Computing (IJESC) **7**(4) (2017)
6. https://en.wikipedia.org/wiki/Toyota_Fortuner
7. Reddy, N., et al.: Switched Quasi Impedance-Source DC-DC Network for Photovoltaic Systems. Int. J. Renew. Energy Res. **13**(2), 681–698 (2023). https://www.ijrer.org/ijrer/index.php/ijrer/article/view/14097
8. http://www.letsrun.com/forum/flat_read.php?thread=3371381
9. https://comparativegeometrics.wordpress.com/2015/12/10/road-gradient-1-definition-and-vehicle-performance/
10. Venkata Govardhan Rao, K., et al.: Design of a bidirectional DC/DC converter for a hybrid electric drive system with dual-battery storing energy. Front. Energy Res. **10**(November) (2022). https://doi.org/10.3389/fenrg.2022.972089
11. Rao, K.V.G., Kiran Kumar, M., Srikanth Goud, B.: An Independently Controlled Two Output Half Bridge Resonant LED Driver. Electr. Power Components Syst. **0**(0), 1–21 (2023). https://doi.org/10.1080/15325008.2023.2238695
12. http://www.trunsunsolar.com
13. Malla, S.G., Bhende, C.N.: Enhanced operation of stand-alone "Photovoltaic-Diesel Generator-Battery" system. Electric Power Systems Research **107**, 250–257 (2014)
14. Bhende, C.N., Malla, S.G.: Novel control of photovoltaic based water pumping system without energy storage. Int. J. Emerg. Electr. Power Sys. **13**(5) (2012)
15. Malla, S.G., Bhende, C.N., Mishra, S.: Photovoltaic based water pumping system. International Conference on Energy, Automation, and Signal (ICEAS), 1–4 (2011)
16. Khare, A., Rangnekar, S.: Optimal Sizing an SPV/Diesel/Battery Hybrid System for a Remote Railway Station in India. Int. J. Renew. Ener. Res. **3**(3) (2013)
17. Betka, A., Moussi, A.: Performance optimization of a photovoltaic induction motor pumping system. Renewable Energy **29**, 2167–2181 (2004)
18. A Report on: Utilisation of Hybrid Energy Services in Island and Rural Communities: Indian and European Scenario. http://www.teriin.org/opet/reports/hybrid.pdf
19. http://www.energymatters.com.au/renewable-energy/solar-power/pumping/
20. Sera, R.T., Hantschel, J., Knoll, M.: Optimized maximum power point tracker for fast-changing environmental conditions. IEEE Trans. Indus. Electro. **55**(7), 2629–2631 (2008)
21. Handbook of Secondary Storage Batteries and Charge Regulators in Photovoltaic Systems Final Report, prepared by Exide Management and Technology Company. West College Avenue, Yardley, Pennsylvania (1981). http://www.azsolarcenter.org/images/docs/tech-science/papers/batteries/start.pdf
22. Aneesha, K., Das, P.G.: A non isolated high step up DC to DC converter with continuous input current for PV system. Int. J. New Technol. Sci. Eng. (IJNTSE) **5**(3), 1–11 (2018)
23. Nisha, C.K., Priya, S.: Bidirectional DC-DC converter for energy storage systems. Int. J. New Technol. Sci. Eng. (IJNTSE) **5**(3), 12–21 (2018)
24. Kopylov, I.P.: Mathematical models of electric machines, translated from the russian by P.S. Ivanov, Revised from the Russian edition (1980)